Under normal steady state operating conditions only pellet pore diffusion limitation and external heat transfer resistance have to be considered. This means isothermal pellet with possible internal concentration profiles. External mass transfer limitations and pellet temperature gradients need only be considered for severe operating conditions. But in this region where the possibility of multiple steady states exists, the reactor is controlled by dynamic factors and is extremely sensitive to variations in operating conditions.

2.2.3.3. Model parameters

The parameters needed for the packed bed reactor models are the kinetic expressions related to the catalyst and chemical reaction system and parameters describing the effective transport properties of the bed and of the individual catalyst particles. Effective transport properties of the bed are described by effective diffusivities and effective conductivities, and transfer of heat to the coolant is described by a heat transfer coefficient at the wall.

Traditional transport models for packed beds assume that the void fraction and the velocity across the reactor is uniform, even along the solid surfaces. They further assume that radial dispersion is constant and not influenced by the reactor wall, except in the close vicinity of the wall where the boundary conditions are employed. However, the assumptions of uniform conditions across the reactor have been questioned lately, due to substantial discrepancies found between simulated and experimental data. This will be revealed in the next chapters.

The transport properties of the pellets are described by effective diffusivities of species in the pores and an effective thermal conductivity of the pellet which includes conductivity in the solid material and conductivity in the fluid phase inside the pores. In addition mass and heat transfer coefficients for the stagnant fluid surrounding the particles may be needed.

The values of the transport parameters are either obtained by fitting the model to experimental data or by using correlations from the litterature. These correlations are mostly based on an empirical or semiempirical approach and correlates dimensionless groups containing effective parameters with dimensionless groups describing the fluid–dynamics and characteristic bed

properties and dimensions. The correlations are often derived from a simplified model of the bed and the transport processes in the bed, and often contain unknown parameters which are determined from experimental data. When parameter values are reported, these are most often determined from experiments under non reacting conditions, and does not allways give a very accurate description of reacting systems.

Quite a large number of correlations are published with a large scatter in accuracy and the range of validity is often restricted. Whether correlations may be used or parameters must be determined from experiments, must be judged from the accuracy needed and the limitations of a lumped mechanism dispersion model's ability to represent a real reaction system under the conditions of interest. Generally correlations or literature values may be used when they have a satisfactory accuracy, or for parameters which do not need to be accurately known. This is the case when the model output are insensitive to variations in the parameter value. The need for accurate values of certain key parameters must be stressed, e.g. effective radial conductivity, but deviations between simulations and experimental data may often be attributed to poorly known kinetics or varying catalyst activity in the reactor due to varying degree of deactivation.

2.2.3.3.1. Dispersion coefficients

The dispersion coefficients for heat and mass are generally given by correlations between fluid–mechanical Peclet numbers, Pe^*, and the Reynolds number, Re_p, to account for turbulent diffusion and mixing, and by the conductivity or diffusivity at stagnant fluid condition. The effective dispersion coefficient is the sum of the dynamic and the static contributions. This relationship is given by equation 2–15 for mass and by equation 2–16 for heat.

$$\frac{1}{Pe_m} = \frac{D_e^0/D_m}{Pe_m^0} + \frac{1}{Pe_m^d} \qquad (2\text{–}15)$$

$$\frac{1}{Pe_h} = \frac{\lambda_e^0/\lambda_g}{Pe_h^0} + \frac{1}{Pe_h^d} \qquad (2\text{–}16)$$

The static contribution to effective thermal conductivity, λ_e^0, consists of a number of individual mechanisms involving both the fluid phase and the solid phase as shown in Table 2–1. The estimation of this parameter is usually based on a simplified geometrical model of the packed bed with resistances acting in series and in parallel. Some of the different correlations are reviewed by Lemcoff et al. (Lemcoff et al., 1990). The correlations may be semi–empirical expressions derived from simple models (Krupiczka, 1967; Lemcoff et al., 1990) or they may be derived from more elaborate models. The most importante correlations of the last kind are the series–parallel resistance model of Kunii and Smith (Kunii and Smith, 1960) and the cell model of Zehner and Schlünder (Zehner and Schlünder, 1970; Bauer and Schlünder, 1978).

The correlations are generally dependent on the conductivities of the fluid and solid phases and on the porosity of the bed. Since the contact area between the particles depends on the geometry of the particles this factor may be taken into account.

The cell model of Zehner and Schlünder (Zehner and Schlünder, 1970; Bauer and Schlünder, 1978) analyzes the heat conduction in an unit cell containing two particles with a contact surface surrounded by fluid. By combining resistances they derived the following expression for the effective stagnant conductivity:

$$\frac{\lambda_c^0}{\lambda_g} = 1 - \sqrt{1-\varepsilon} + \sqrt{1-\varepsilon}\frac{2}{1-Bx}\left[\frac{(1-x)B}{(1-Bx)^2}\ln\frac{1}{Bx} - \frac{B+1}{2} - \frac{B-1}{1-Bx}\right] \qquad (2\text{–}17)$$

$$B = C\left(\frac{1-\varepsilon}{\varepsilon}\right)^{10/9} \qquad x = \frac{\lambda_g}{\lambda_p}$$

The form factor C in equation 2–17 is dependent on particle geometry and is 1.25 for spheres

and 2.5 for cylinders. The void fraction, ϵ, may be a mean value across the bed, or may be dependent on reactor position. In the last case λ^0_e becomes dependent on reactor position.

At higher temperatures the effect of conduction by radiation may be incorporated in equation 2–17, and at lower pressures the Smoluchowski effect may be taken into account (Bauer and Schlünder, 1978).

The effective molecular diffusivity in the bed is affected by the porosity and the tortuosity of the bed (Doraiswamy and Sharma, 1984). Zehner and Schlünder (Zehner and Schlünder, 1970) derived the following expression for the effective diffusivity from their cell model:

$$\frac{D^0_e}{D_m} = 1 - \sqrt{1-\epsilon} \qquad (2\text{–}18)$$

The fluid–mechanical Peclet numbers have different values for axial and radial directions, but are principally equal for heat and mass transfer because of the convective nature of the transport. They decrease with increasing Reynolds number reaching a constant value at higher Reynolds numbers as shown in Figure 2–7.

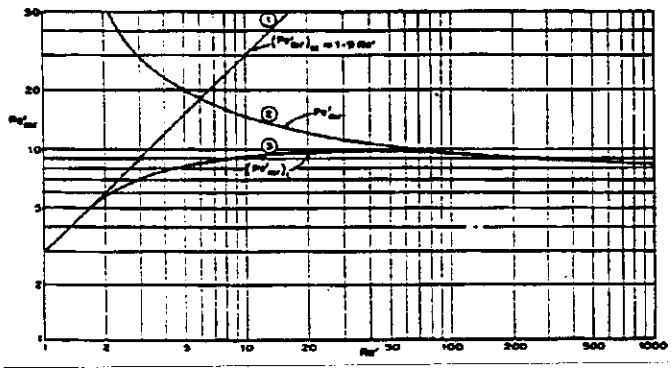

Figure 2–7. The total effective, $(Pe'_{ax})_e$ turbulent, Pe'_{ax}, and molecular, $(Pe'_{ax})_m$, Peclet numbers as function of Reynolds number.
From Kulkarni and Doraiswamy, 1980.

The effective Peclet numbers are obtained by combining molecular and turbulent diffusion, and their dependence on Reynolds number are shown in Figure 2–7. They increase proportionally with increasing Reynolds number at low Reynolds numbers due to the independence of molecular diffusion on flow, possibly reaching a maximum at some Reynolds number e.g. (Gunn, 1967; Dorweiler and Fahien, 1959). At higher Reynolds numbers the effective Peclet numbers reach the constant values of the fluid–mechanical Peclet numbers. In this flow regime mass dispersion and thermal conductivity increase proportional to increase in superficial velocity.

To account for the Peclet numbers dependence of the Reynolds number, empirical correlations of the form of equation 2–19 and 2–20 have been presented both for axial and radial dispersion. These equations predict the observed maximum in the Peclet number versus Reynolds number relationship. The equation coefficients are usually determined from experimental data and are usually different for radial and axial dispersion and for heat and mass. Reviews and discussions of different correlations are given by e.g. (Kulkarni and Doraiswamy, 1980; Doraiswamy and Sharma, 1984; Lemcoff et al., 1990; Dixon and Cresswell, 1979; Freiwald and Paterson, 1992).

$$\frac{1}{Pe_m} = \frac{C_1}{1+\frac{C_2}{Re_p Sc}} + \frac{C_3}{Re_p Sc} \qquad (2\text{–}19)$$

$$\frac{1}{Pe_h} = \frac{C_1}{1+\frac{C_2}{Re_p Pr}} + \frac{C_3}{Re_p Pr} \qquad (2\text{–}20)$$

The difference in Peclet number values for axial and radial dispersion is attributed to differences in the mechanisms causing dispersion. According to Sundaresan et al. (Sundaresan et al., 1980) axial mixing in the voids occurs but there is no real axial dispersion. Gunn (Gunn, 1969) models axial dispersion as a tendency of the fluid particles to be "held up" in the bed thus resulting in a probabiliy of movement. This probability is a measure of the extent

of fast fluid stream through the reactor while the rest of the stream moves only by molecular diffusion. By inclusion of mass transfer between the two streams an expression for the effective Peclet number was obtained as a function of Reynolds number and Schmidt number and the probability of movement. But this probability is dependent on Reynolds number and could only be calculated from experimental data. At higher Reynolds numbers the probability was shown to approach 0.5 giving an axial Peclet number of approximately 2.

Radial dispersion may be described as random deflection of fluid elements within a cell structure of particles (Schlünder, 1966) or by a random walk model (Baron, 1952). Schlünder (Schlünder, 1966) obtained a theoretical value of 8 for the fluid–mechanical Peclet number in the bulk and 16 within the distance of a particle diameter from the wall. The higher value of the Peclet number in the near–wall region is attributed to the resistance to radial mixing in this region induced by the rigid wall. This result was derived from a simplified flow model and shows that the mean radial Peclet number is correlated to the d_p/d_t ratio according to the relationship shown in equation 2–25. The results of Schlünder are consistent with experimental data which shows that the radial Peclet number varies with axial position (Fahien and Smith, 1955).

Correlations of the type 2–19 and 2–20 are often simplified by neglecting the dependence of the fluid–mechanical Peclet number on flow conditions, using the asymptotic values valid at higher Reynolds numbers. Vortmeyer and Haidegger (Vortmeyer and Haidegger, 1991) recommended the following correlations for heat and mass dispersion based on this approach. A correction is made for the wall effect for radial dispersion.

$$\frac{1}{Pe_{mz}} = \frac{1-\sqrt{1-e_0}}{Re_p Sc} + \frac{1}{2} \qquad (2\text{-}21)$$

$$\frac{1}{Pe_{mr}} = \frac{1-\sqrt{1-e_0}}{Re_p Sc} + \frac{1}{1.1 Pe_r^d} \qquad (2\text{-}22)$$

$$\frac{1}{Pe_{hz}} = \frac{\lambda_d^0/\lambda_g}{Re_p Pr} + 0.7 \qquad (2\text{-}23)$$

$$\frac{1}{Pe_{hr}} = \frac{\lambda_d^0/\lambda_g}{Re_p Pr} + \frac{1}{Pe_r^d} \qquad (2\text{-}24)$$

where

$$Pe_r^d = 8\left[2-\left(1-\frac{2d_p}{d_t}\right)^2\right] \qquad (2\text{-}25)$$

is the theoretical relationship obtained by Schlünder (Schlünder, 1966).

Dixon and Cresswell (Dixon and Cresswell, 1979) obtained semianalytical correlations for the effective radial and axial conductivities based on a collocation–perturbation technique solution of the dispersion model equations. These correlations differ from the correlations discussed so far, and are dependent on the wall heat transfer coefficient and the fluid–solid heat transfer coefficient.

2.2.3.3.2. Heat transfer coefficients

The concept of heat transfer coefficients in a packed bed reactor is attributed to layers of stagnant fluid separating solid surfaces and mixing zones. This is supposed to occur at the reactor wall and between the solid particles and the bulk fluid, creating additional resistance to heat transfer in this regions. The heat transfer coefficients are usually correlated to the fluid dynamics in term of a Nusselt versus Reynolds number relationship.

Some of these correlations are reviewed by e.g. (Lemcoff et al., 1990), and the great scatter between predictions of Nu_w from different published correlations are shown by e.g. (Dixon and Cresswell, 1979; Tsotsas and Schlünder, 1990; Vortmeyer and Haidegger, 1991). These confusions have led to a number of different correlations, typically restricted to a certain range of the Reynolds number, a range of the tube diameter to particle diameter ratio and to a certain particle shape.

The scatter are particulary pronounced for $Re_p < 1000$ leading Tsotsas and Schlünder (Tsotsas and Schlünder, 1990) to suggest that for this range of the Reynolds number the concept of a heat transfer resistance at the wall is physically incorrect, and that the wall heat transfer coefficient α_w is a lumped parameter accounting for all effects that have been neglected in the model equations. These include the variations in void fraction, fluid velocity and thermal conductivity near the wall, and small systematic errors in experimental data. Such errors are very important in connection with long tubes where thermal equilibrium is closely approximated.

Dixon and Cresswell (Dixon and Cresswell, 1979) explain the great scatter in the Nusselt versus Reynolds number relationship by the presumption that the wall heat transfer coefficient is not a unique function of Reynolds number and fluid conductivity, but should rather be correlated to the effective radial conductivity. This would take into account the effect of solid heat transfer and solid–wall heat transfer, the void fraction of the bed and the near wall restrictions on the effective fluid phase conductivity. From these assumptions Dixon and Cresswell conclude that a Biot versus Reynolds number correlation is more correct than a Nusselt versus Reynolds number correlations. They have shown that a Biot number correlation gives considerably less scatter than a Nusselt number correlation for particles of different shapes and different d_t/d_p ratio.

Dixon and Cresswell (Dixon and Cresswell, 1979) have proposed the following correlation for estimation of the wall heat transfer coefficient based on the particle diameter Biot number.

$$Bi_w = 3.0\ Re_p^{-0.25} \qquad (2\text{–}26)$$

The fluid–solid heat transfer coefficient is also commonly correlated by a Nusselt versus Reynolds number relationship, but for low values of the Reynolds number there is a great scatter between different correlations. Dixon and Cresswell (Dixon and Cresswell, 1979) have recommended the following correlation.

$$Nu_c = (0.255/\epsilon)\ Pr^{1/3}\ Re_p^{2/3} \qquad (2\text{–}27)$$

for $Re_p > 100$ and $d_t/d_p > 8$.

2.2.4. Radial heat transfer in packed beds – Conflicts of evidence

The effective radial conductivity and the wall heat transfer coefficient are the most important transport parameters in traditional dispersion models. While simulated concentration and temperature profiles are relatively insensitive to variations in mass dispersion parameters and axial conductivity, the profiles are strongly dependent on the values of the radial thermal conductivity. This is particulary true for reaction with a high heat production potential.

Estimation of accurate values for the radial heat transport parameters is, however, difficult for two reasons. One is the great scatter in predictions made from available correlations, and the other is the observed differences in estimated effective radial conductivity under reactive and non–reactive conditions. The influence of chemical reaction on effective radial conductivity has been reported in several publications (Hofmann, 1979; Paterson and Carberry, 1983; Schwedock et al., 1989b). The tendency is that the radial conductivity has to be increased for exothermic reacting systems compared to non–reacting systems in order to give an acceptable fit between observed and simulated temperature profiles.

This last observation has raised the question of the physical correctness of the traditional dipersion models, or if chemical reaction in some way influences the heat transport properties of the bed. The latter veiw is, however, not very likely, so the answer probably lies in the model structure.

Wijngaarden and Westerterp (Wijngaarden and Westerterp, 1989) argue that the discrepancy

is due to the use of a homogeneous model when a heterogeneous model should be used. A heterogeneous model distinguishes between pellet and fluid temperature while a homogeneous model uses the fluid temperature for the calculation of reaction rates. For an exothermic reaction where pellet temperature is higher than fluid temperature, a homogeneous model will predict lower reaction rates and heat production and thus underestimate temperature gradients. From this view a compensation is suggested by decreasing the radial conductivity to obtain more profound profiles. This is, however, contradictory to most experimental observations, and Wijngaarden and Westerterp argue that this is due to the use of inaccurate correlations for the estimation of heat transport parameters.

The findings of Schwedock et al. (Schwedock et al., 1989b) was that the radial conductivity had to be increased both for the homogeneous and heterogeneous model under reactive conditions compared with measurements at non–reactive conditions. The measurements at reactive and non–reactive conditions were performed in the same reactor under comparable flow conditions. The results also showed that the apparent radial conductivity increased with increasing conversion without any significant differences between the homogeneous and the heterogeneous model. From this it is not likely that the dispute concerning radial heat transfer in packed beds can be explained from differences in homogeneous and heterogeneous models. But in cases where pellet temperature differs substantially from fluid temperature, the heat transfer resistance between the pellets and the fluid phase has to be taken into account.

It is more likely that the explanation of the confusion regarding radial heat transfer in packed beds lies in the modeling of the packed bed structure and the mechanisms of conduction. The traditional dispersion models assume radial uniformity of all parameters and a distinct heat transfer resistance at the wall caused by a layer of unmixed fluid. However, these assumptions have been contradicted by the following findings and theories:

1. The void fraction of the bed is not uniform but tends to increase towards the reactor wall reaching a value of 1 at the wall.
2. Due to this void fraction profile, the velocity is not constant across the bed but varies according to the variation in void fraction and to the boundary conditions at the wall.
3. The radial dispersion coefficients are functions of velocity, and therefore show radial

variations.

4. The rigid wall causes reduced mixing intencity in the near–wall region due to reflection of stream lines. This causes reduced dispersion in this region.
5. Questions have been put forward as to the nature of heat transfer at the wall. It has been argued that there is no distinct heat transfer restistance at the wall for smaller values of the molecular Peclet number, typical for fixed bed reactor operations.

These issuses will be further revealed in the next chapters.

2.2.5. Radial nonuniformity in packed beds

2.2.5.1. Void fraction

Although the nonuniform structure of packed beds has been known for a time, this topic has only lately received attention in connection with the modeling of fixed bed reactors. The void fraction in a bed with spherical particles oscillates in a damped fashion, decreasing from unity at the wall to a constant value in the interior of the bed (Benenati and Brosilow, 1962) as shown in Figure 2–8. Perfectly shaped spheres show the most regular oscillation pattern while for irregularly shaped spheres and other geometries the oscillation pattern is less pronounced or completely absent. Lerou and Froment (Lerou and Froment, 1986) have measured void fraction profiles in packed beds for spheres and Raschig rings, and their results are shown in Appendix IV. Although the Raschig rings show no particular oscillations, the void fraction is unity at the wall and constant in the interior of the bed.

To incorporate a radial void fraction profile in the reactor models, some descriptions or models reflecting at least the main features of the profile are necessary. A rather detailed model of the structure of the packing of spherical particles from the wall to the interior of the bed in tubular reactors has been developed by Froment et al. (Govindarao and Froment, 1986; Delmas and Froment, 1988). A much simpler relation has been used by Vortmeyer and Schuster (Vortmeyer and Schuster, 1983) for calculation of radial velocity profiles in beds packed with spherical particles. This relation which is given by equation 2–28 and depicted

in Figure 2–8, reflects the main features of the void fraction profile and are frequently used by others. It describes the profile by an exponential decaying function and do not show the oscillatory behaviour. A cosinus–function may be incorporated to account for this (Küfner and Hofmann, 1990).

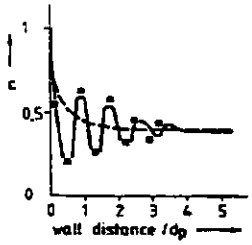

Figure 2–8. Porosity distribution for spherical particles near the wall; ——, averaged porosity function calculated from equation 2–28. From Vortmeyer and Schuster, 1983.

$$\varepsilon = \varepsilon_\infty \left[1 + C e^{\left(1-2\frac{R-r}{d_p}\right)} \right] \qquad (2\text{–}28)$$

The constant C in equation 2–28 has to be adjusted according to the condition: ε=1 at r=R.

2.2.5.2. Velocity

The radial velocity profile in packed beds depends on the variations in void fraction across the bed. Vortmeyer and Schuster (Vortmeyer and Schuster, 1983) have used the Brinkman equation extended with the Ergun pressure loss relation to calculate velocity profiles in packed beds with assumed void fraction profiles according to equation 2–28. Their momentum balance equation is shown in equation 2–29. A similar expression was used by Delmas and Froment (Delmas and Froment, 1988) in a study of the effect of radial nonuniformities on velocity and effective heat and mass transfer coefficients. However, in their momentum balance the coefficients f_1 and f_2 differed somewhat from the expressions

shown in equations 2–31 and 2–32.

$$\frac{\partial P}{\partial z} = -f_1 v - f_2 v^2 + \mu_g \frac{1}{r}\frac{\partial}{\partial r}(r\frac{\partial v}{\partial r}) \qquad (2\text{–}29)$$

Boundary conditions of equation 2–29:

$$\frac{\partial v}{\partial r} = 0 \qquad \text{at } r = 0 \qquad (2\text{–}30a)$$

$$v = 0 \qquad \text{at } r = R \qquad (2\text{–}30b)$$

The factors f_1 and f_2 in equation 2–28 are:

$$f_1 = 1.75\rho_g \frac{1-e}{e^3 d_p} \qquad (2\text{–}31)$$

$$f_2 = 175\rho_g \frac{1-e}{e^3 d_p} \qquad (2\text{–}32)$$

For an isothermal bed the radial velocity profile originates from the dependence of the factors f_1 and f_2 on local void fraction, and from the non–slip boundary condition of equation 2–30b. The axial flow in packed beds is characterized by a pronounced by–pass near the wall and a reduced flow in the centre as shown in Figure 2–9.

Vortmeyer and Schuster (Vortmeyer and Schuster, 1983) have obtained velocity profiles for isothermal flow, using equation 2–29. A number of different flow conditions were evaluated, and the results were used to adapt a semi–analytical expression to the profiles calculated from equation 2–29. Thus an analytical expression for the radial flow profile applicable for different flow conditions and tube diameter to particle diameter ratios, was obtained. This expression is shown in Appendix IV.

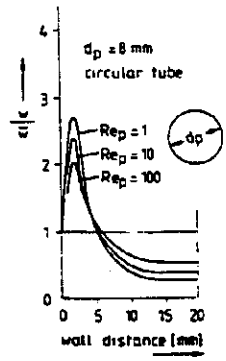

Figure 2–9. Calculated dimensionless flow profiles for a circular packed bed. From Vortmeyer and Schuster, 1983.

The effect of non–isothermal conditions on velocity profile can at first hand be estimated by allowing fluid density and viscosity in equation 2–29 to vary with temperature. In wall cooled tubular reactors there are, however, often profound radial temperature variations with subsequent variations in fluid density. These variations in density may induce radial mass fluxes in the bed. In this case both the axial and radial momentum equations and the continuity equation are needed in addition to the conventional energy and mass balances. All these equation are coupled, and must be solved simultaneously.

The interactions between temperature and flow for a wall cooled reactor with an exothermic reaction have been analyzed by Vortmeyer et al. (Vortmeyer et al., 1992). They conclude that models which include the interaction between temperature and fluid density tend to predict higher temperatures than models which do not include this interaction. But the difference compared with a model which includes the radial void fraction profile and isothermal velocity profile was not very large.

These conclusions are supported by a similar work of Daszkowski and Eigenberger (Daszkowski and Eigenberger, 1992). They conclude that the build–up of the flow profile takes place in the first particle layer through a strong radial flow component. Thereafter the radial component reduces to zero, and the axial flow profile stays constant. Furthermore, they

conclude that the mass flux profile is not much affected by radial temperature gradients.

The main problem concerning the verification of the influence of the radial void fraction profile and the temperature profile on the velocity profile is the difficulties of measuring the gas flow inside the packing. Since this is almost impossible without disturbing the flow, reliable flow measurements can only be obtained above or below the packing. Vortmeyer and Schuster (Vortmeyer and Schuster, 1983) have compared their simulations with the measured data of Schwartz and Smith (Schwartz and Smith, 1953) and found some substantial differences. This is attributed to the distortion of velocity profiles between the exit plane of the bed and the actual plane where the measurements were taken. Daszkowski and Eigenberger (Daszkowski and Eigenberger, 1992) have also measured velocity profiles below the bed, but they extended their flow model to include this region. From this, they found reasonable agreement between measured and computed velocity profiles.

2.2.5.3. Radial dispersion

The radial nonuniformities of porosity and velocity in packed beds and the reduced mixing intencity in the near–wall region are all factors which may influence the dispersion of heat and mass. The effect is that the values of the dispersion coefficients become dependent on reactor position, contradictory to traditional dispersion models which assume that the values are independent of reactor position. If dispersion coefficients vary with reactor position, this will introduce additional errors and physically incorrectness in traditional models. This may at least partially explain the discrepancies found between heat transfer parameters estimated under reacting and non–reacting conditions and the great scatter in prediction of dispersion parameters from different correlations.

Both the radial variation in velocity and the reduced mixing intencity in the near–wall region have been taken into account in estimating the radial dependency of the dispersion coefficients. The effective radial Peclet number has been shown experimentally to depend on radial position (Fahien and Smith, 1955). A theoretical estimation of the wall effect has been reported by Schlünder (Schlünder, 1966) using a simplified cell model. He found that the

value of the fluid–mechanical Peclet number in the region of one particle diameter from the wall was twice the value at the interior of the bed, obtaining an expression for the mean radial Peclet number shown in equation 2–25. Another approach is to introduce a wall function as in the classical turbulent–flow theory where the turbulent dispersion increases proportionally with increasing distance from the wall in the near–wall region (Cheng and Vortmeyer, 1988; Hunt and Tien, 1988).

The effect of radial variations in velocity is usually estimated by taking the fluid–mechanical contribution to the dispersion coefficients proportional to the local velocity (Delmas and Froment, 1988; Cheng and Vortmeyer, 1988; Hunt and Tien, 1988). Whether corrections should be made both for the velocity and the wall effect, or for velocity only, remain at the time open. Tsotsas and Schlünder (Tsotsas and Schlünder, 1988) have shown that predictions of the mean fluid–mechanical Peclet number by equation 2–25 (Schlünder, 1966) correlates well with predictions performed by using the analytical expression for the radial flow profile from Vortmeyer and Schuster (Vortmeyer and Schuster, 1983) without any additional wall function. Agreement between predictions and experimental data was reported to be good too.

Another uncertain factor in the introduction of a wall function is the extent of the region where such a function eventually is physically correct. Cheng and Vortmeyer (Cheng and Vortmeyer, 1988) have found the proportionality between dispersion and distance from the wall to extend up to 2.5 particle diameters from the wall while Hunt and Tien (Hunt and Tien, 1988) have assumed it to extend only up to one particle diameter from the wall.

The most important parameter where an accurate knowledge of the radial dependency is required, is the effective radial conductivity as the model output is most sensitive to variations in the value of this parameter. Correlations relating the radial conductivity to local velocity and distance from the wall have been proposed by Cheng and Vortmeyer (Cheng and Vortmeyer, 1988) and Hunt and Tien (Hunt and Tien, 1988). These correlations can be expressed by the general form shown in equation 2–33 with the wall function defined by equation 2–34. Different values for the constants C_1 and C_2 used in the equations were reported in the two publications, as well as a somewhat different relation for the calculation of the radial dependence of the effective conductivity of the bed with stagnant fluid, λ^0_e. The

radial dependence of this parameter is due to the radial variations in void fraction which alters the relative importance of solid phase and fluid phase conductivity.

Equation 2–33 predicts that the effective radial thermal conductivity decreases towards the wall reaching the value of the fluid thermal conductivity at the wall. This is due to zero velocity and a void fraction of unity at the wall.

The effective radial thermal conductivity is correlated by:

$$\frac{\lambda_r(r)}{\lambda_g} = \frac{\lambda_e^0(r)}{\lambda_g} + C_1 Re_p Pr \frac{v(r)}{v_0} f(R-r) \qquad (2\text{–}33)$$

with the following expression for the wall function:

$$f(R-r) = \begin{cases} \dfrac{R-r}{C_2 d_p} & for\ 0 \le (R-r) \le C_2 d_p \\ 1 \quad for\ (R-r) > C_2 d_p \end{cases} \qquad (2\text{–}34)$$

The wall function increases linearly up to a distance of C_2 particle diameters from the wall.

2.2.6. Heat transfer at the wall

In traditional dispersion models heat transfer at the wall is modeled using a wall heat transfer coefficient. The temperature–slip boundary condition is

$$-\lambda_{er} \frac{\partial T}{\partial r} = \alpha_w (T - T_w) \qquad (2\text{–}35)$$

This approach is physically correct only if heat transfer at the wall is inhibited by a thin layer of unmixed fluid with a higher heat transfer resistance than in the interior of the bed. The correctness of such an approach has been questioned (Tsotsas and Schlünder, 1990; Hunt and Tien, 1990; Vortmeyer and Haidegger, 1991), and Tsotsas and Schlünder have pointed out that a distinct heat transfer resistance only exists at higher molecular Peclet numbers in

packed beds. In the region of Peclet numbers usually encountered in fixed bed reactor operations no such heat resistance exists, and the heat transfer coefficient parameter α_w is only a lumping parameter having to mathematically compensate the influence of several effects. Among these effects are the radial nonuniformities of the fluid velocity and dispersion coefficients.

The great scatter in experimentally determined values of α_w for the flow regime typical for industrial fixed bed processes is attributed to the use of incorrect boundary conditions. Heat transfer in this area proceeds through normal conduction, and an appropriate boundary condition for this situation should be used. This may be a constant temperature condition or a heat conduction boundary condition.

2.2.7. Summary – The wall heat conduction model

It is generally agreed that radial void fraction and velocity profiles exist in packed beds, and that the use of local velocity in the model equations gives significant improvements compared to traditional models using mean velocity.

To which extent the radial thermal conductivity should be modified, and the question of correct boundary conditions for heat transfer at the wall is more uncertain. More research is evidently needed in this area.

Vortmeyer and Haidegger (Vortmeyer and Haidegger, 1991) have proposed a model taking into account the factors discussed above. Their model which they call the wall heat conduction model, uses local velocity calculated from the expression of Vortmeyer and Schuster (Vortmeyer and Schuster, 1983) shown in Appendix IV. The reaction rates are corrected for local variations in void fraction, and they use a radial dependent effective thermal conductivity calculated from equation 2–33. The other dispersion coefficients are considered less important, and they use constant values for those, calculated from equations 2–21 to 2–23. Heat fluxes at the wall are modeled using a heat conduction boundary condition by including heat conduction through the wall.

Balance equations and boundary conditions for the heat conduction model are shown below. A simplification has been done in the wall heat balance equation 2–37 by neglecting axial temperature gradients in the reactor wall. The notation is according to the symbol list and Figure 2–6.

The equations of the pseudo–homogeneous wall heat conduction model are:

heat balance reactor

$$(1-e)\rho_g C_{pg}\frac{\partial T}{\partial t} = -v\rho_g C_{pg}\frac{\partial T}{\partial z} + \lambda_{ax}\frac{\partial^2 T}{\partial z^2} + \frac{1}{r}\frac{\partial}{\partial r}(r\lambda_r\frac{\partial T}{\partial r}) + \rho_b\frac{(1-e)}{(1-e_0)}\eta(-\Delta H)r_v \qquad (2\text{–}36)$$

heat balance wall

$$\lambda_w\frac{1}{r}\frac{\partial}{\partial r}(r\frac{\partial T}{\partial r}) = 0 \qquad (2\text{–}37)$$

mass balance

$$0 = -v\frac{\partial C_i}{\partial z} + D_{ax}\frac{\partial^2 C_i}{\partial z^2} + D_{ar}\frac{1}{r}\frac{\partial}{\partial r}(r\frac{\partial C_i}{\partial r}) + \rho_b\frac{(1-e)}{(1-e_0)}\eta r_{v,i} \qquad (2\text{–}38)$$

Initial conditions

at t = 0, all z and r

$$T(z,r) = T^0(z,r) \qquad (2\text{–}39)$$

Boundary conditions

at t > 0

$$\frac{\partial T}{\partial r} = \frac{\partial C_i}{\partial r} = 0 \qquad \text{at r = 0, all z} \qquad \text{(2–40a)}$$

$$\lambda_r \frac{\partial T}{\partial r} = \lambda_w \frac{\partial T}{\partial r} \qquad \text{at r = R, all z} \qquad \text{(2–40b)}$$

$$\frac{\partial C_i}{\partial r} = 0 \qquad \text{at r = R, all z} \qquad \text{(2–40c)}$$

$$-\lambda_w \frac{\partial T}{\partial r} = \alpha_c (T - T_c) \qquad \text{at r = R}_o\text{, all z} \qquad \text{(2–40d)}$$

$$\lambda_\infty \frac{\partial T}{\partial z} = \nu \rho_g C_{pg} (T - T_0) \qquad \text{at z = 0, all r} \qquad \text{(2–40e)}$$

$$D_\infty \frac{\partial C_i}{\partial z} = \nu (C_i - C_{0,i}) \qquad \text{at z = 0, all r} \qquad \text{(2–40f)}$$

$$\frac{\partial T}{\partial z} = \frac{\partial C_i}{\partial z} = 0 \qquad \text{at z = L, all r} \qquad \text{(2–40g)}$$

2.3. FISCHER TROPSCH KINETICS

2.3.1. Reactions and stoichiometry

The composition of the reaction product from the Fischer–Tropsch synthesis is kinetically controlled rather than thermodynamically (Mc Ketta, 1985). This implies that the product spectrum is determined by the relative rates of all the reaction steps involved on the catalytic surface.

The main products from the Fischer–Tropsch synthesis over cobalt–based catalysts are n–alkanes and 1–alkenes (Yates and Satterfield, 1991). Branched alkanes and alkenes are only produced in minor quantities on conventional Fischer–Tropsch catalysts. The stoichiometry of the main reactions are:

$$nCO + (2n+1)H_2 \rightarrow C_nH_{2n+2} + nH_2O \qquad (2\text{–}41)$$

$$nCO + 2nH_2 \rightarrow C_nH_{2n} + nH_2O \qquad (2\text{–}42)$$

Depending on catalyst properties and operating conditions the alkene content of the product mixture may vary from almost nothing to the major constituent. Generally the alkene content increases with decreasing H_2/CO ratio (Dry, 1981).

Considerable amounts of oxygenated products, mainly alcohols but also aldehydes, ketones and carboxylic acides, may be formed over cobalt and iron catalysts especially at lower temperatures (Dry, 1981). But under normal operating conditions the content of oxygenates in the product from a cobalt catalysed Fischer–Tropsch synthesis is usually low. At 473 K organic oxygenates typically constitute about 1 percent of the total organic product (Gall et al., 1952).

In addition to the reactions leading to the formation of organic products the water gas shift reaction and the Boudouard reaction leading to carbon deposition may occur.

$$CO + H_2O \rightarrow CO_2 + H_2 \qquad (2\text{–}43)$$

$$2\,CO \rightarrow C + CO_2 \qquad (2\text{–}44)$$

Whereas iron catalysts have a high shift activity, neither the shift reaction nor reactions leading to the deposition of carbon seem to take place to any significant extent on cobalt based Fischer–Tropsch catalysts under normal operating conditions (Dry, 1981).

2.3.2. Reaction mechanism

The Fischer–Tropsch synthesis is from a mechanistical view rather complex with a diverse product spectrum and a numerous possible reacting intermediates on the catalytic surface. Therefore, several different mechanisms have been proposed, and the question about the correct mechanism has been discussed since the discovery of the reaction.

It is generally accepted that the build up of longer carbon chains occurs through a polymerization mechanism where monomer is inserted in the chain at the bond between a carbon and a surface site. But regarding the mechanism of formation and structure of the monomer several theories have been put forward. The monomer is generally belived to be a C_1 species formed by reaction between CO and H but mechanisms involving insertion of longer carbon chains have also been proposed. While it is generally agreed that H_2 adsorbs dissociatively on the metal surface, the question whether CO dissociates in the process of monomer formation is more unclear.

Reaction schemes and discussions of the various proposed mechanisms have been reviewed by several authors e.g. (Dry, 1981; Biloen and Sachtler, 1981; Anderson, 1984; Schanke, 1986). There are three main theories for the mechanism where two involves oxygen containing intermediates and the third assumes that a CH_x carbidic species is the building block in the formation of higher hydrocarbons.

In the mechanism put forward by Storch, Golumbic and Anderson an oxymethylene HCOH

species is postulated as the basic buildig block. The carbon chain is formed by condensation of such species. A C–C bond is then formed by eliminating water. In the CO insertion mechanism proposed by Pichler and Schulz (Pichler and Schulz, 1970) CO adsorbed on the surface is inserted directly in the growing carbon chains, and then the oxygen is removed by hydrogenation liberating water. In both these mechanisms the carbon attached to the surface is oxygenated and thus the formation of oxygenated products can easily be explained.

The carbide insertion theory is the oldest originally proposed by Fischer but has been refined and extended later and is now the most accepted theory. The insertion element is a partially hydrogenated carbon atom, preferably CH_2. This means that CO has to be dissociated and partially hydrogenated before insertion. Many studies indicate that CO adsorps dissociatively under normal reaction temperatures forming carbon on the surface. This carbon is reactive and can be hydrogenated to form the insertion species. Evidence for this is given by experimental data from e.g. Ekerdt and Bell (Ekerdt and Bell, 1979) who observed the formation of hydrocarbons when purging the reactor with hydrogen after treatment with CO. The hydrocarbon formation continued after all adsorbed CO, detectable by infrared spectroscopy, had disappeared. This suggests that there are substantial amounts of carbon buildt up on the surface during steady state operation and this carbon is reactive in hydrogenation reactions. But it was also observed that under steady state operations a substantial amount of undissociated chemisorbed CO was present on the surface. This is not so easily explained from experimental evidence showing that CO dissociation is a fast reaction. Biloen and Sachtler (Biloen and Sachtler, 1981) say that this is indicative of an ensemble effect. CO dissociation needs an ensemble of free surface active points in order to occur and can only take place on a limited part of the surface.

Simplifications in the development of reaction mechanisms are often made. This may be that only formation of the main products is accounted for, but a fully developed Fischer–Tropsch reaction mechanism should be able to describe the formation of all the product observed as well as their carbon number distribution. This means that the possibility of branching should be included in the chain propagation mechanism.

One of the weaknesses of the carbide insertion theory is the difficulty of explaining the formation of oxygenates. To account for this Dry (Dry, 1981) has proposed a general reaction scheme including elements from both the carbide insertion theory and the CO insertion theory. This scheme is shown in Figure 2–10. Another extension of the carbide insertion theory has been made by Wojciechowski (Wojciechowski, 1988). Here oxygenates are formed by termination reactions involving different oxygen containing species.

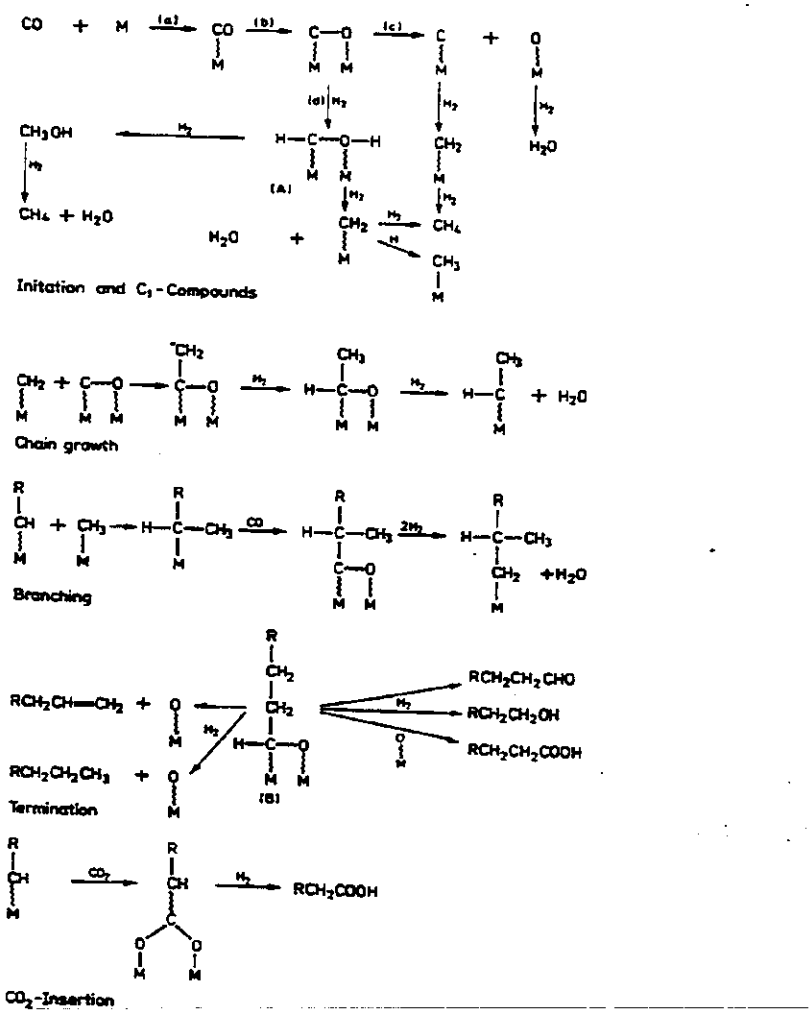

Figure 2–10. A general Fischer–Tropsch reaction scheme. From Dry, 1981.